01 Sep 1969

Turbulence Measurements in Shear Flow Liquid Systems

Robert S. Brodkey

M. F. Cohen

J. S. Knox

G. L. McKee

TURBULENCE MEASUREMENTS IN SHEAR FLOW LIQUID SYSTEMS *

Robert S. Brodkey**, M. F. Cohen, Capt. J. S. Knox, G. L. McKee
K. N. McKelvey, M. A. Rao, S. Zakanycz, and H. C. Yieh
The Ohio State University
Columbus, Ohio

ABSTRACT

The paper is a composite of a number of years of work on turbulence measurements in a variety of liquid flow systems. The trials and tribulations of such measurements are emphasized. Pipe flow is considered in some detail, and the consistency between results of various investigators is analyzed. Other systems discussed are a stirred tank unit and a multi-jet reactor configuration. Statistical turbulence measurements such as autocorrelation, spectrum, probability density, flatness factor, and skewness factor are considered in terms of obtaining these from digital signals obtained by conversion of the normal analog signals. Descriptive parameters of statistical turbulence, such as microscale, macroscale, and kinetic energy dissipation, are discussed, as well as various attempts at the estimation of these without using statistical turbulence measurements.

INTRODUCTION

During the past twelve years, we have extensively investigated turbulent motion mixing, and kinetics. This work has been presented in a number of papers and reviews[1-9]. During the course of these studies we have measured the turbulence characteristics of liquid flows in a number of systems. Most extensively studied was pipe flow, but measurements have also been made in a stirred mixing vessel and a multijet injector reactor configuration. The present paper presents these results together with empirical estimation of some of the parameters involved. The experimental equipment is for the most part conventional with minor modifications made for convenience of measurement. Our basic system is a Lintronic Model 40.

TURBULENT PIPE FLOW OF LIQUIDS

The most extensive measurements of shear flows are those made in boundary layers and in pipes. Because of the importance of pipeline mixing, we have concentrated our attention on the latter. The most common measurements for such turbulence are the components of the Reynolds stress tensor, and of these, the most commonly measured is the axial intensity of turbulence. One means of representing such data is to plot the relative intensity at the center-line as a function of the Reynolds number. However, since we considered only one Reynolds number (50,000 based on the center-line velocity or 40,600 as normally measured), we will avoid this plot and simply say that our results were within the spread of data reported in the literature, which range from 2.7 to 3.9 per cent. Our most reliable value[24] of 3.4 per cent is the same as that of Laufer[10] for air flow in a large pipe system. This check should not be construed to imply that measurements in liquids can be considered as accurate as those in air.

When we first started our mixing studies[7], we were primarily concerned with water flows. We made turbulence measurements[7,22] but these were at best approximate because of calibration drift, which was a result of contamination by rust particles and high water conductivity. Because of this, attempts to measure the other Reynolds stresses were to no avail[22]. There are routes which can be taken to eliminate the probe drift problem. First, one can use extremely clean water in an extremely clean system or second, one can abandon water and use an organic liquid. An organic liquid loop had already been built (the loop used for the visual studies discussed elsewhere); consequently, the fluid in that system, trichloroethylene, was used as the test liquid. These[23] and the measurements by Patterson[14] are the only organic liquid results available.

More information about the flow can be obtained from the axial turbulent intensity distribution across the radius of the pipe. Results of the present study[23,24] and those of other authors are presented in Figure 1. Most are at about the same Reynolds number we used. Over the limited range of variation in Figure 1, no systematic tendency with Reynolds number is apparent. The tendencies of all runs are similar with deviation between results becoming more pronounced as the wall region is approached. The precision for any given run is considerably higher than the accuracy between runs. The investigators cited all have taken reasonable precautions to insure fully developed flow. Care and understanding of the equipment used was obvious in all cases and the deviation between results is unexplained. The deviation in the air runs is of the same order as in liquids. The liquid results average less than the gas results, but the differences in the averages is about the same as the deviations in either the air or liquid results. Since the gas flow systems were larger and since hot-wire anemometry was used rather than hot-film or visual methods, it would appear that the gas results are more reliable. First, more is known about the heat transfer from hot-wires than from hot-films. Second, a larger system allows much more accurate positioning and less interference from probe mounts. If it were necessary to select one set of measurements as the most reliable, those of Laufer[10] are probably the best, and are near the average for the gas and liquid results combined.

Measurement of the other components of the Reynolds stress tensor would be most interesting, but the techniques involved are more difficult, thus fewer measurements have been reported. Two measurements inclined at $\pm\ \theta^{o}$ at one position are needed. We first used a V-shaped probe with two films at $\pm$ 30° in the trichlorethylene system.[23] The analysis of the results involved taking the difference of the two readings to get the cross stress and the difference of the sum of the two readings with another term calculated from the axial intensity to get u'_r and u'_θ. With two probes, we could not calibrate accurately enough to obtain completely satisfactory data. As a final effort[24], we used a single 30° inclined probe which we could rotate through the four positions. This made the results much closer to a point measurement and involved only a single calibration. In Figure 2, our results and those of others are presented. One should not be surprised that the agreements between results are only marginal when one considers the agreement for the easier to measure u'_x shown in Figure 1. The high results for liquids are a direct consequence of the low values of the axial intensity. As mentioned, the radial and tangential components are calculated from the difference of two large numbers, one of which depends directly on the axial intensity.

The cross flow terms, $\overline{u_x u_r}$, of the Reynolds stress satisfied the theoretical relation

*Supported in part by the U.S. Air Force and by NSF grants.
**Professor of Chemical Engineering.

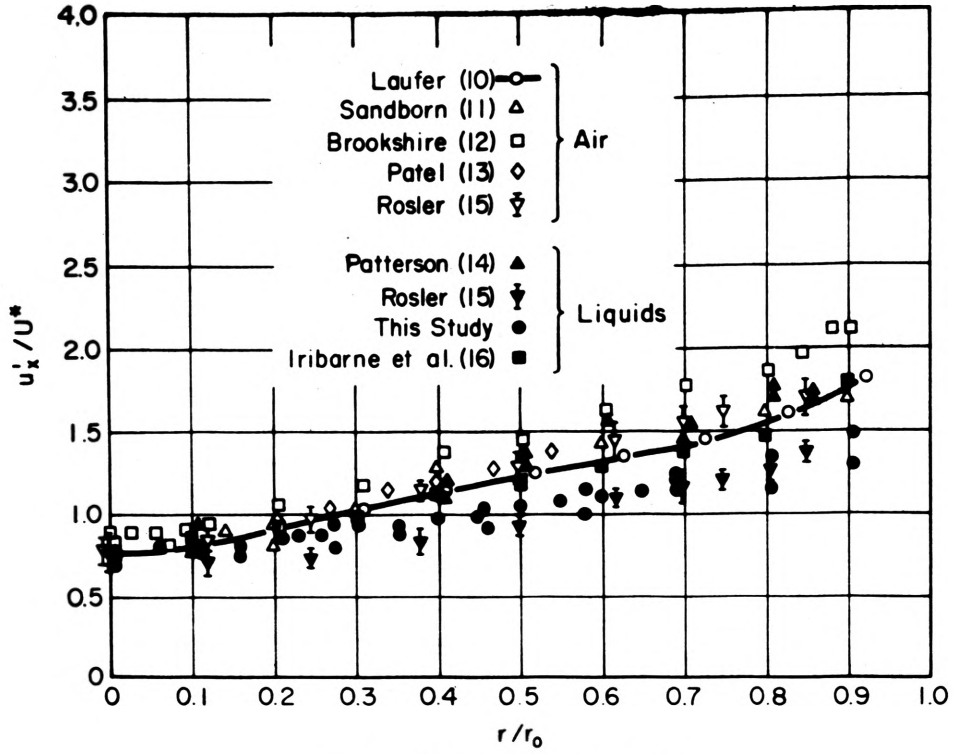

Fig. 1. Axial Turbulent Fluctuation Data

$$\frac{r}{r_o} U^{*2} = -\nu \frac{d\bar{U}_x}{dr} + \overline{u_x u_r} \qquad (1)$$

obtained from the Reynolds equation, as it did for others when measured. Thus all of these results are internally consistent. The cross stress term, $\overline{u_r u_\theta}$, can be theoretically shown to be zero. The final cross stress term, $\overline{u_x u_\theta}$, has been measured only twice, by Brookshire[12] for an air flow and in this work[24]. Results are consistent with each other, being approximately one third of the corresponding axial intensity. However, these results are most unreliable as they involve the difference of large numbers.

It should be apparent that the measurement of the components of the Reynolds stress and their distribution in pipe flow is a matter not completely resolved. For our part, we would rely on the principle of similarity as put forth by Reynolds and the measurements of Laufer to give what we think are the best values available. The measurements in liquid systems do give the appearance of a major deviation from corresponding gas results, but a careful investigation of Figures 1 and 2 indicates this may be only a superficial difference. But one should keep an open mind on the subject as better measurements become

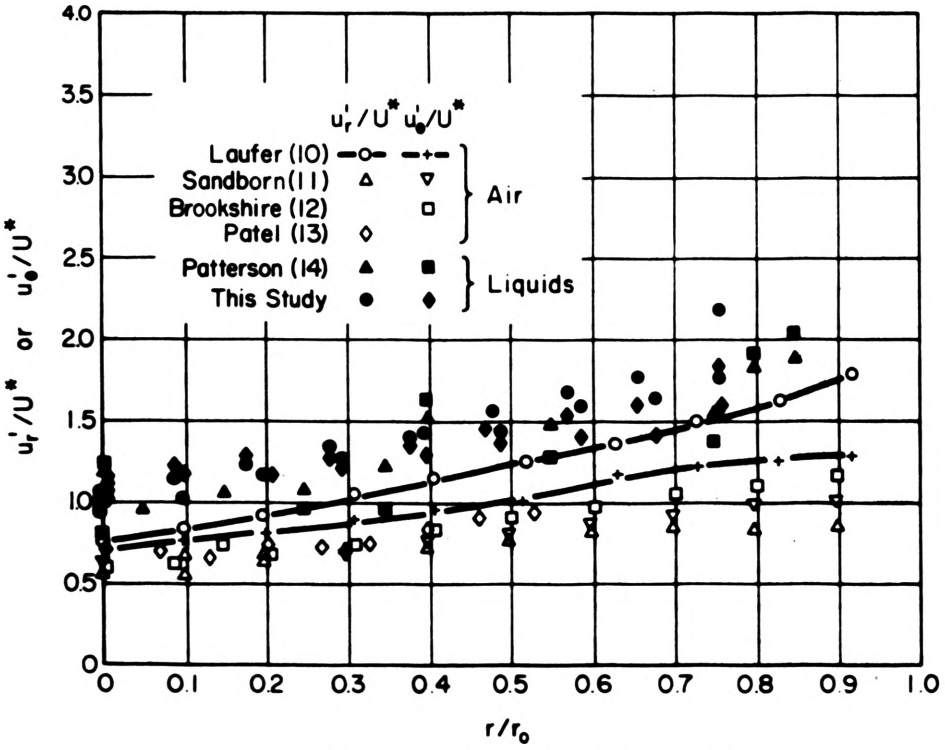

Fig. 2. Radial and Tangential Turbulent Fluctuation Data

available. More study is in order on methods of measurements particularly for hot films such as the recent investigation by Bellhouse and Schultz (17).

TURBULENT FLOW IN OTHER SYSTEMS

In pipe flow the direction of the mean velocity vector is well defined, and the necessary orientation of a Pitot tube or hot-film aneometer follows directly. In a system like a mixing vessel, the velocity vector direction is unknown and must first be established before turbulence measurements can be made and related to the coordinates of the vessel[25]. We will not go into great detail about our results, but we do want to emphasize the aforementioned point, since it has been ignored by several investigators. One further point missed by others is that Pitot tube measurements of the magnitude of the velocity vector will be incorrect in very high turbulence regions because of the high turbulence level and the inadequacy of correction methods for this.

We chose to use a multiport null type Pitot tube of standard commercial design (United Sensor Inc.) to establish the velocity vector direction and uncorrected magnitude. The actual magnitude was determined with an orientated hot-film probe. The vessel configuration is shown in Figure 3. One example of the uncorrected mean velocity from the Pitot tube together with the mean velocity from the independently calibrated hot-film are shown in Figure 4. Note that these are the vector magnitudes and the directions vary with position. It is an easy matter to resolve these into system coordinates as the direction is also known.[25] The intensity of turbulence in the velocity vector direction is shown in Figure 5. The relative intensity was fairly uniform being between 48 and 65%, which can be compared to the 3.4% at the center-line in pipe flow. As pointed out by Hinze[18], there is no adequate correction method that could correct the Pitot tube magnitudes to those of the hot film. Clearly one must take extreme precautions when measuring turbulence properties in undefined velocity direction fields and fields with high turbulent intensities.

One final measurement problem was uncovered in making turbulence studies on the multi-jet injection reactor[26]. The system geometry can induce extreme non-isotropic conditions. By extreme non-isotropic conditions we mean that even the crude condition of $u'_x = u'_r = u'_\theta$ at the center-line is not approximately met. The geometry is identical to that of Vassilatos and Toor[19], and is shown in Figure 6. Photographs and more detail are in reference 9. On logical grounds, the system should have provided a uniform flow field with a relatively flat velocity profile at the start, slowly changing into the turbulent parabolic form as the flow proceeded down the pipe beyond the injectors. This is what we thought. But this was not exactly what we found. Instead of a flat profile, there were vorticies along the wall, which were associated with the back flow in the region near the wall. This back flow caused considerable change in the mean velocity and all other aspects of the flow. The net result was a complex flow, far more complicated than expected. In Figure 7, the center-line axial velocity is plotted against axial position and, instead of a uniform flow, there is a very rapid and then a slower decrease. This is associated with a jetting effect which the back flow on the wall induces. Figure 8 shows the intensity of the velocity fluctuations at the centerline as a function of axial

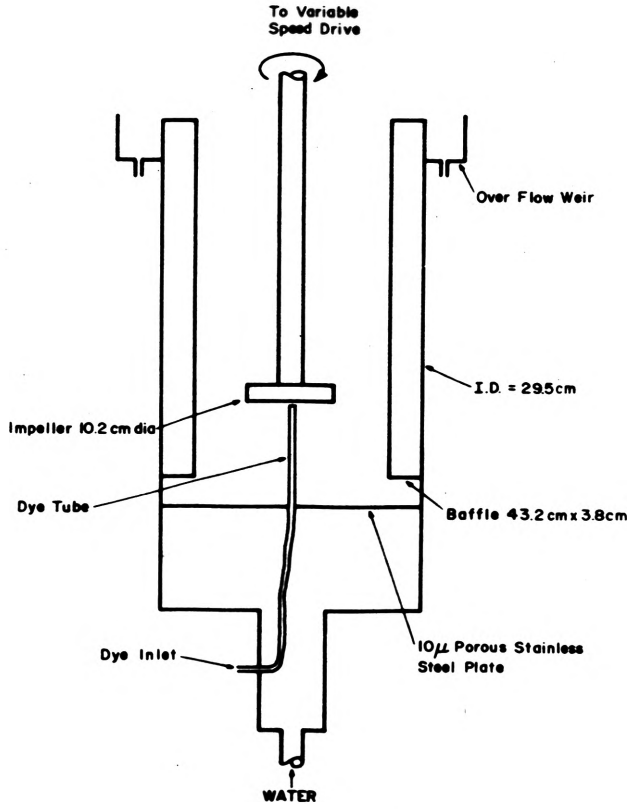

Fig. 3. Stirred Tank Flow System

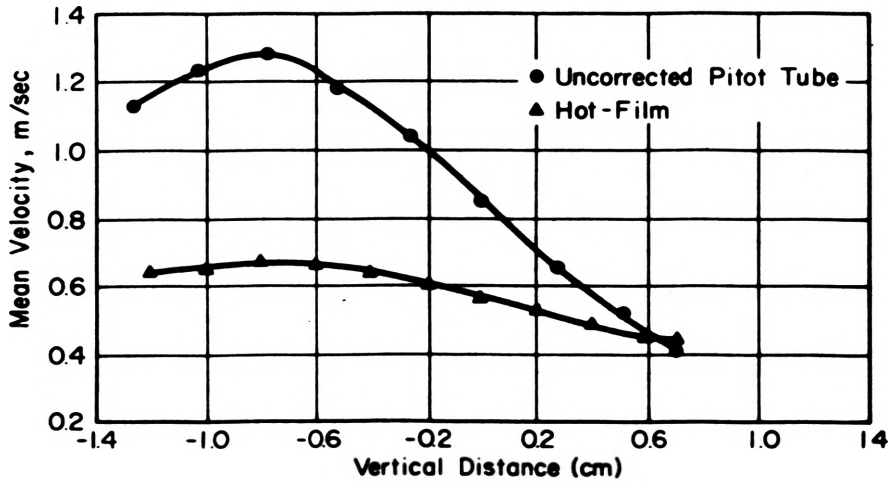

Fig. 4. Pitot Tube Measurements Compared to Hot-Film Results at 0.5-inch from Impeller

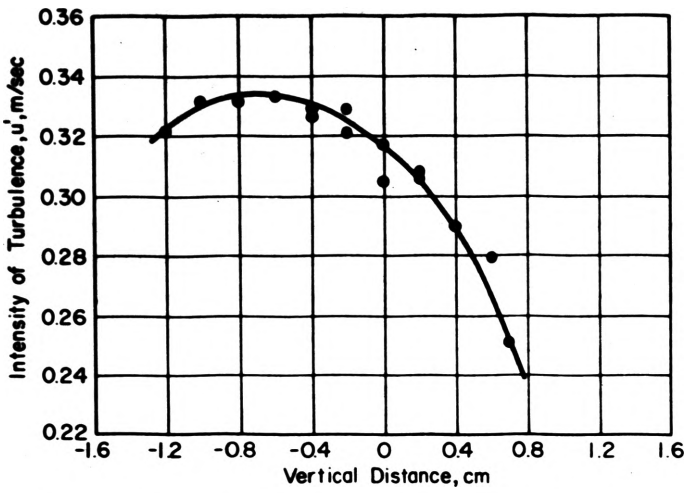

Fig. 5. Distribution of the Intensity of Turbulence at 0.5-inch from Impeller

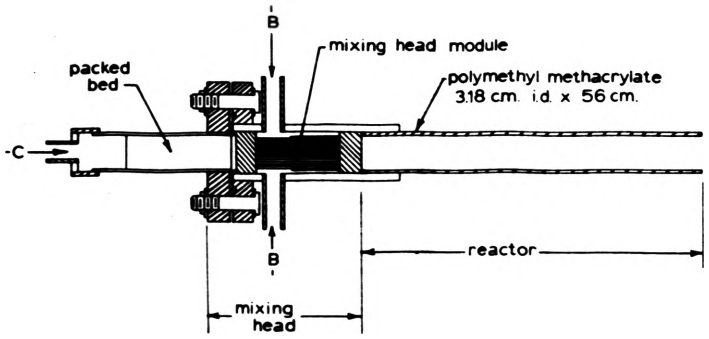

Fig. 6. Multi-jet Injector Reactor Configuration

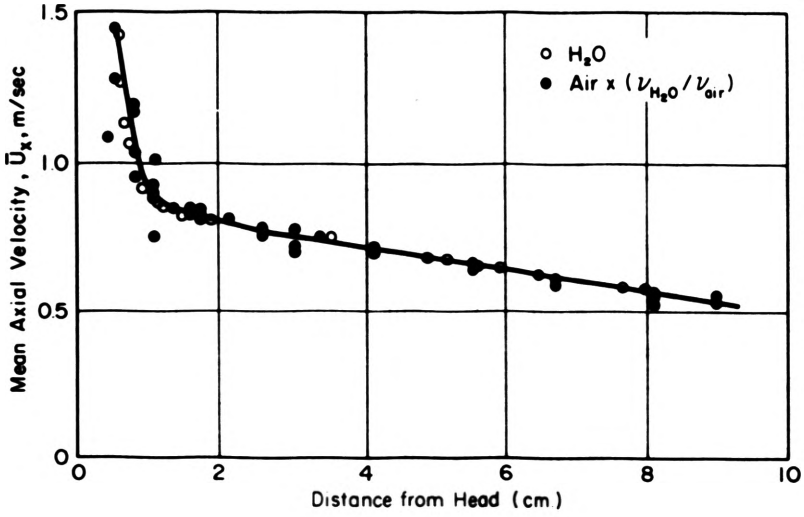

Fig. 7. Mean Axial Velocity

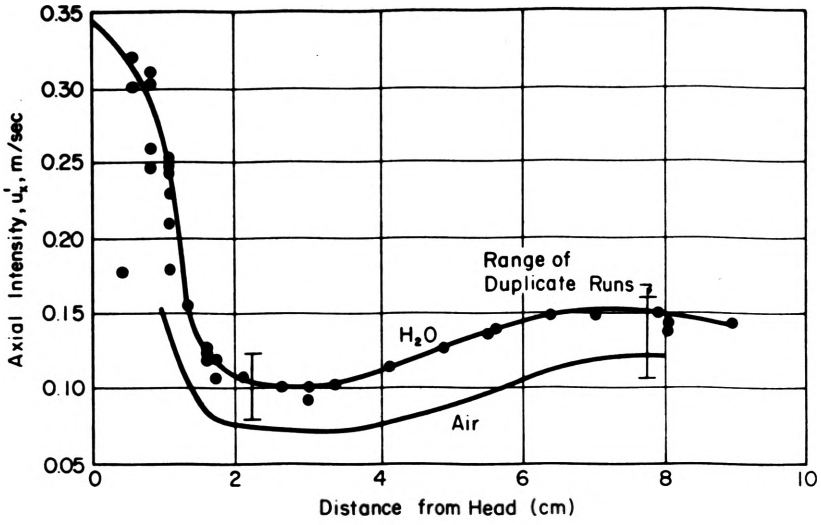

Fig. 8. Axial Intensity of Turbulence

position. There is a rapid decrease in intensity following the injection from the small tubes, a minimum occurs, and then an increase to an equilibrium value results. The minimum is unusual but is associated with the jet effect.

On an identical air system[27], in which we could make more reliable radial measurements, we have found that the increase in energy was associated with the vortex or a separation that occurs near the wall. Furthermore, we have obtained high-speed movies[28] of the flow as a function of axial distance and the difference in the appearance of the field from the minimum axial intensity region to far from the head is dramatic. In potentially complex fields, the simple measurement of an axial intensity may not be an adequate description of the turbulence.

STATISTICAL TURBULENT MEASUREMENTS

By the parameters of statistical turbulence, we mean those descriptive terms obtained by processing the instantaneous signal beyond just the rms value. For the most part, such analysis has been restricted to turbulence in the axial direction. There have been some measurements in other than the axial direction. These are most difficult to make, and have been mainly concerned with the establishment of true isotropic conditions in certain flow systems. We have studied the axial characteristics only.

The most common measurement on the fluctuating signal have been spectra evaluation by analog methods. Figure 9 is a composite of ours[7,24,26] and many other measurements. Because of the number, no attempt has been made to distinguish the results by different authors. The -5/3 upper region is from the isotropic conditions used by Grant et al.[20] Results that fall off to the left are in non-isotropic shear flows. The lower results at high wave numbers are from Lee and Brodkey[7]. Agreement for $k/k_\eta > 0.1$ illustrates that nearly all spectra exhibit a universal equilibrium range at high wave numbers regardless of the fact that the flow may be anisotropic. The low frequency end of the spectra show deviations from the isotropic estimations in a manner characteristic of the forces generating the turbulence.

Some autocorrelation evaluation has been done by using time delay by means of a tape recorder (i.e., ref. 14). We were fortunate to have available an analog to digital converter (Radiation Inc. A2D, 375 to 40,000/sec.) and

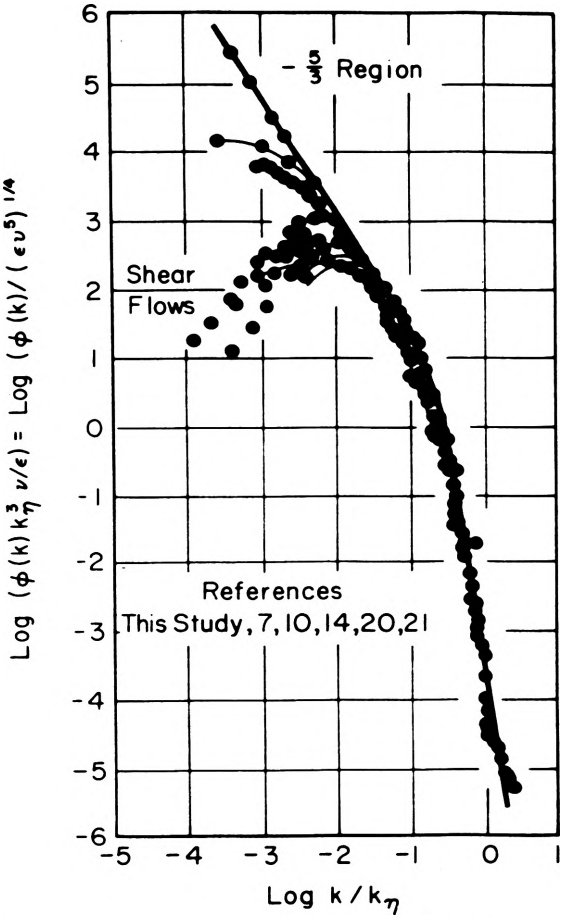

Fig. 9. Normalized Spectrum as a Function of Normalized Wave Number

large digital computers (IBM 7094, 360-75) to process the signals. We developed our own autocorrelation and subsequent conversion to spectrum programs[26]. More recently we have also made use of a fast Fourier transform program to obtain spectra directly from the digitized information[28]. Probability distribution analysis was also incorporated into our autocorrelation program.

The normalized autocorrelation is defined as

$$f(\tau) = \frac{\overline{u_x(t)u_x(t+\tau)}}{\overline{u_x(t)^2}} \tag{2}$$

and was first estimated at discrete times, $\tau = n\Delta t$, by

$$f(n\Delta t) = \frac{\frac{1}{N}\sum_{i=1}^{N} [u_x(i\Delta t)\, u_x(i\Delta t + n\Delta t)]}{\frac{1}{N}\sum_{i=1}^{N} [u_x(i\Delta t)]^2} \tag{3}$$

where N is a suitably large number. However, this equation could not be used satisfactorily because the signal reaching the computer had a small d.c. component. Some of this signal is known to come from the tape recorder. The correlation obtained then is the correlation of the signal, $s = a\, u_x + \bar{s}$ or

$$\frac{\overline{s(t)\, s(t+\tau)}}{\overline{s(t)^2}} = \frac{\overline{s(t)^2} + a^2\, \overline{u_x(t)\, u_x(t+\tau)}}{\overline{s(t)^2}} \tag{4}$$

This equation can be rearranged to give the desired normalized autocorrelation

$$f(\tau) = \frac{\overline{u_x(t)\, u_x(t+\tau)}}{\overline{u_x(t)^2}} = \frac{\overline{s^2}}{\overline{s^2} - \bar{s}^2} \frac{\overline{s(t)\, s(t+\tau)}}{\overline{s^2}} - \frac{\bar{s}^2}{\overline{s^2} - \bar{s}^2} \tag{5}$$

where $\bar{s}$ and $\overline{s^2}$ are estimated by

$$\bar{s} = \frac{1}{N}\sum_{i=1}^{N} s(i\Delta t)\,; \quad \overline{s^2} = \frac{1}{N}\sum_{i=1}^{N} [s(i\Delta t)]^2 \tag{6}$$

where N is a suitably large value. The desired autocorrelation can be calculated from Equation (5) with the uncorrected autocorrelation,

$$\frac{\overline{s(t)\, s(t+\tau)}}{\overline{s^2}}$$

calculated from Eq. (3) with s replacing u_x. An example[26] of such an autocorrelation calculated by this technique is shown in Figure 10.

An oscillation in the autocorrelation is an indication of a preferred frequency (or crudely eddy size). For example near the impeller in a stirred tank the autocorrelation oscillates about zero at exactly the frequency of the blades passing the hot-film sensor[25]. Further removed these oscillations are damped out. Indeed, close to any normally used turbulence generating device, the autocorrelation will help detect the fundamental frequency of the system and can be used to determine when these characteristics of individual systems are damped out by viscous forces.

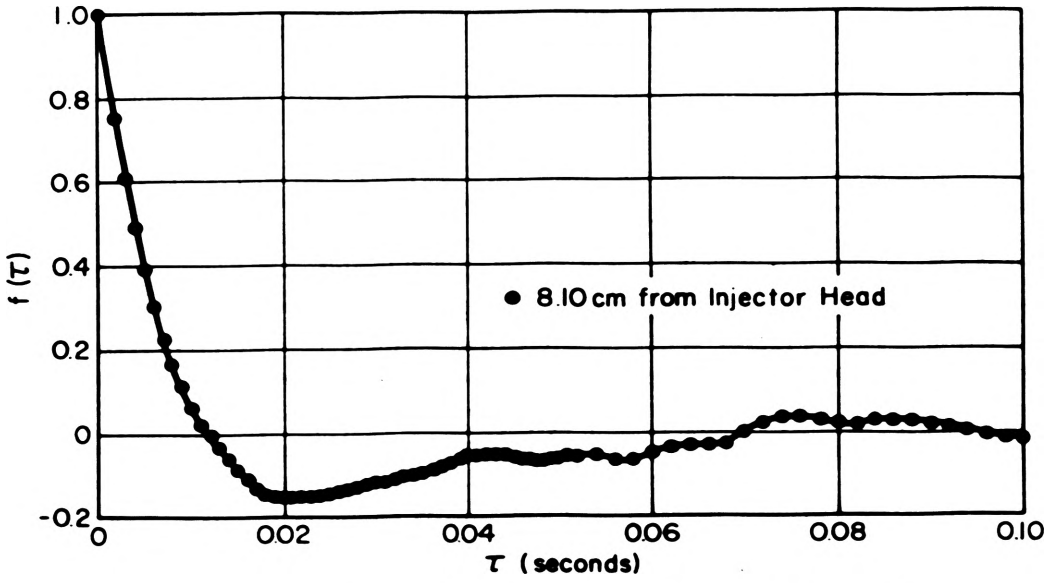

Fig. 10. Velocity Autocorrelation, 8.1 cm from Injector Head

The one-dimensional velocity spectrum, $\phi(k)$ and the autocorrelation are related by the transform equations

$$\phi(k) = \frac{1}{\pi} \int_0^\infty \overline{u_x^2}\, f(r_x) \cos(kr_x)\, dr_x \tag{7}$$

and

$$\overline{u_x^2}\, f(r_x) = 2 \int_0^\infty \phi(k) \cos(kr_x)\, dk \tag{8}$$

where Taylor's hypothesis, $r_x = \bar{U}_x \tau$, has been assumed valid.

Some spectra were computed[26] by Equation (7). The first temptation is to integrate this equation by one of the usual numerical techniques; however, more careful examination reveals that this is not a wise approach. For large values of k the integrand of Equation (7) oscillates rapidly, and to integrate this numerically would require extremely small increments in r_x. In order to bypass this difficulty, an equation is first fitted to $f(r_x)$; then the integration can be carried out analytically.

Since $f(r_x)$ is a smooth, well behaved function, it can easily be represented by a simple equation. A second order equation was chosen to represent $f(r_x)$ between each two points, $r_{x,i-1}$ and $r_{x,i}$:

$$f(r_x) = A_i r_x^2 + B_i r_x + C_i \quad \text{for} \quad r_{x,i-1} \le r_x \le r_{x,i} \tag{9}$$

The values of the constants A_i, B_i, and C_i were chosen so that the curve passed through the points $[f(r_{x,i-1}), r_{x,i-1}]$ and $[f(r_{x,i}), r_{x,i}]$ and so that the differences between the predicted and experimental values at $r_{x,i-2}$ and $r_{x,i+1}$ were a minimum in the least squares sense. This last condition causes the curvature of the function between $r_{x,i-1}$ and $r_{x,i}$ to be directed by the values at $r_{x,i-2}$ and $r_{x,i+1}$. The one dimensional velocity spectrum was then integrated as

$$\begin{aligned}
\phi(k) &= \frac{\overline{u_x^2}}{\pi} \sum_{i=2}^{N} \int_{r_{x,i-1}}^{r_{x,i}} (A_i r_x^2 + B_i r_x + C_i) \cos(kr_x)\, dr_x \\
&= \frac{\overline{u_x^2}}{\pi} \sum_{i=2}^{N} \left[A_i \int_{r_{x,i-1}}^{r_{x,i}} r_x^2 \cos(kr_x)\, dr_x + B_i \int_{r_{x,i-1}}^{r_{x,i}} r_x \cos(kr_x)\, dr_x \right. \\
&\quad \left. + C_i \int_{r_{x,i-1}}^{r_{x,i}} \cos(kr_x)\, dr_x \right] \\
&= \frac{\overline{u_x^2}}{\pi} \sum_{i=2}^{N} \left[\frac{A_i}{k^2} (2kr_x \cos kr_x + (k^2 r_x^2 - 2) \sin k_x r_x) \right]_{r_{x,i-1}}^{r_{x,i}} \\
&\quad + \frac{B_i}{k^2} (\cos kr_x + kr_x \sin kr_x) \Big]_{r_{x,i-1}}^{r_{x,i}} \\
&\quad + \frac{C_i}{k} \sin kr_x \Big]_{r_{x,i-1}}^{r_{x,i}}
\end{aligned} \tag{10}$$

The spectra, $\phi(k)$, computed by Eq. (10) are included in Figure 9.

In addition to describing the turbulent field in a time domain as an autocorrelation and in a frequency domain as an energy spectrum, it is possible to describe the field in a probability domain as a probability density of the velocity fluctuations. The probability density is estimated by

$$P(u_x) = \frac{\text{Prob.}\,[u_x \le x \le (u_x + \Delta u_x)]}{\Delta u_x} \tag{11}$$

where Δu_x is suitably small. Due to the presence of the small d.c. component, the value of $\bar{u}_x$ defined as the first moment

$$\bar{u}_x = \int_{-\infty}^{+\infty} u_x P(u_x)\, du_x \tag{12}$$

was not equal to zero, as required by definition. The $\bar{u}_x$ calculated from Equation (12) was subtracted from the velocities. The corrected values of the velocities were also used to evaluate[25] the flatness factor, $F(u_x)$, and the skewness factor, $S(u_x)$, defined respectively as:

$$F(u_x) = \frac{\int_{-\infty}^{\infty} u_x^4 P(u_x)\, du_x}{\left[\int_{-\infty}^{\infty} u_x^2 P(u_x)\, du_x\right]^2} = \frac{\overline{u_x^4}}{\left[\overline{u_x^2}\right]^2} \tag{13}$$

and

$$S(u_x) = \frac{\int_{-\infty}^{\infty} u_x^3 P(u_x)\, du_x}{\left[\int_{-\infty}^{\infty} u_x^2 P(u_x)\, du_x\right]^{3/2}} = \frac{\overline{u_x^3}}{\left[\overline{u_x^2}\right]^{3/2}} \tag{14}$$

To save space, we will not show these here; suffice it to say that the probability density of the velocity fluctuations was very close to a normal distribution for the reactor configuration[26] and thus for the center-line region of a pipe, but was highly non-normal with a positive skew for the mixing tank[25].

DESCRIPTIVE PARAMETERS OF STATISTICAL TURBULENCE

The main parameters obtained from the autocorrelation and spectrum are microscale, macroscale, and turbulent energy dissipation. These can usually be determined in more than one way, thus offering an internal check on precision of the calculations.

The microscale or dissipation length is defined as

$$\lambda^2 = 1/(d^2 f/dr_x^2)\,\Big|_{r_x=0} \tag{15}$$

or equivalently

$$\lambda^2 = u_x'^2 / \overline{(\partial u_x/\partial r)^2} \tag{16}$$

with

$$\partial u_x/\partial r = (1/\bar{U}_x)(du_x/dt) \tag{17}$$

which is Taylor's hypothesis, or

$$\lambda^2 = \overline{u_x^2} \Big/ 2\int_0^\infty k^2 \phi(k)\, dk \tag{18}$$

Still another method involves the assumption of a normally distributed variable (2):

$$\lambda^2 = \bar{U}_x^2/\pi^2 N(0)^2 \tag{19}$$

where N(0) is the average rate of sign change or the density of zero-crossings. For the reactor configuration[26] the absolute check between Eqs. (15, 16, 18, and 19) was about 5% for positions close to the head and 15% several inches away. The microscale increased as the distance from the head increased, being 0.42 mm at 1.1 cm, 0.91 mm at 3.0 cm, and 1.3 mm at 8.1 cm from the head[26]. The good check using Eq. (19) was to be expected since the velocity fluctuations were normally distributed. For the stirred tank[25], Eqs. (15, 16, and 18) had a maximum absolute deviation of 26% and a minimum of 3% with the average deviation being 13% for all positions studied. Equation (15) was also tested by analog methods and found to check to 13%. Equation (19) gave erratic results as was to be expected since the velocity fluctuations were not normally distributed. An overall average microscale could be taken as 0.82 mm.

In our pipe flow work, the analog tapes were not preserved, so we only had the final spectrum results. Even so, microscales could be calculated directly from the spectrum via Eq. (18) or from the autocorrelation (Eq.15) which in turn was obtained from the spectrum[28]. For a water flow in a 3-inch pipe at our fixed pipe Reynolds number, the value was 2.23 mm at the center-line. For the trichloroethylene flow in a 2-inch line, the values were 1.62,

1.44, 1.19 mm at the center-line, $r/r_o = 0.35$, and $r/r_o = 0.70$, respectively.

The macroscale is defined as

$$L_f = \int_o^\infty f(r_x)\, dr_x \qquad (20)$$

Although the macroscale is strictly defined by Eq. (20), its primary value is as a measure of the large scale fluid motions. In many respects the area L_2 under the normalized correlation function from $r_x = 0$ to the point at which the correlation first becomes negative might be a better measure of this scale (See Fig. 11). Since in general most turbulent fields which have been examined experimentally do not exhibit as strong periodic motions as in our studies, $f(r_x)$ has generally been found to be positive, and $L_f = L_2$. Actually $L_f = L_2 + L_3 + \ldots$ turns out to be a very small number and its value is questionable.[25,26] Even of more value than L_2 would be L_1 defined as $L_1 = |L_2| + |L_3|$ (again see Fig. 11). In the reaction configuration[26], L_f varied from 0.04 to 0.24 mm, which is unreasonably small when compared to 0.42 to 1.3 mm for the microscale. In contrast L_2 varies from 0.90 to 2.66 mm and L_1 from 1.76 to 5.08 mm. The latter values are more reasonable. For the mixing vessel[25], overall average macroscales were $L_f = 0.4$ mm, $L_2 = 2.6$ mm, and $L_1 = 4.48$ mm, again when compared to $\lambda = 0.82$ mm, the latter values appear more reasonable. Thus one would conclude in non-isotropic systems where periodic motions occur, a better definition of a macroscale would be the integration to the first zero crossing or integration of the absolute value of the correlation rather than application of Eq. (20) directly.

For pipe flow the only estimate that could be made was crude and was made from[28]

$$L_f = (\pi/u_x'^2)\phi(0) \qquad (21)$$

For the water flow, $L_f = 14.2$ mm, and for the trichloroethylene flow $L_f = 12.1$, 8.8, and 5.4 mm for the three positions.

The final term is the kinetic energy dissipation, which was determined from the spectrum and from the isotropic relation

$$\epsilon = 15\, \nu\, \overline{u_x^2}/\lambda^2 \qquad (22)$$

By using this relationship we are not assuming that the field is isotropic, but we are expressing our hope that Eq. (22) predicts results which are insensitive to the isotropic assumption. The results of this estimation were made by using the average value of the microscale. Thus this is no better than the microscale estimation.

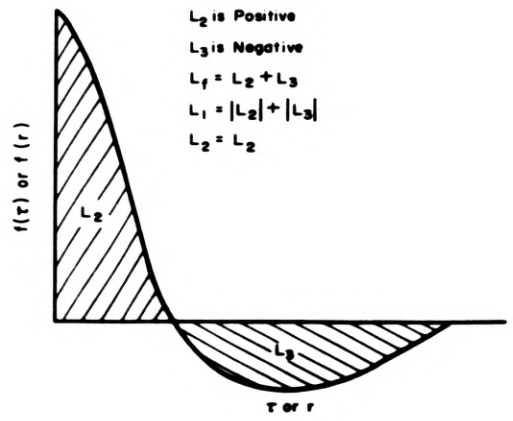

Fig. 11. Macroscales

Other terms of interest are directly dependent on these parameters: Reynolds numbers based on λ, L_f, L_1, L_2; i.e.,

$$N_{Re,\lambda} = \lambda\, u_x'/\nu$$

Kolmogoroff's wave number

$$k_\eta = (\epsilon/\nu^3)^{1/4} \qquad (24)$$

and a lower wave number characteristic of the large velocity eddies

$$k_0 = (2/3)^{3/2}\, \epsilon/u_x'^3 \qquad (25)$$

For pipe flow for later comparison, the values of the parameters were $\epsilon = 16.2$ cm^2/sec^3 and $k_0 = 0.70$ cm^{-1} for the center-line flow of water. For the trichloroethylene ϵ=3.9, 6.8, and 16.1 cm^2/sec^3 for the center-line, $r/r_0 = 0.35$, and $r/r_0 = 0.70$. k_0 for the same three positions was 0.86, 0.94, and 1.07 cm^{-1}.

ESTIMATION OF STATISTICAL PARAMETERS

The various scales, microscales, wave numbers, and dissipation parameters would be most useful if they could be estimated without measurement of autocorrelation or spectrum, as it is these that appear as the controlling parameters of mixing.[1-9] The least complicated system is pipe flow; thus, let us consider this first.[28] Let us assume the only information available is the system (fundamental properties such as ν), geometry, and the rms axial fluctuation, u_x'. The following have been suggested as reasonable but a bit crude estimates:[1,2,5-9]

$$k_0 = 2/r_0 \qquad (26)$$

$$L_f = (3/4)(1/k_0) \qquad (27)$$

$$\lambda^2 = 10\, \nu L_f/1.1\, u_x' \qquad (28)$$

or combining Eqs. (26-28) gives

$$\lambda^2 = 3.41\, \nu r_0/u_x'$$

finally combining Eqs. (22) and (29) gives (29)

$$\epsilon = (15/3.41)(u_x'^3/r_0) \qquad (30)$$

For pipe flow, Eqs. (26) and (30) are compared to the experimental results in Table I, and the agreement is well within what might be expected. For the more complicated flow of the multijet reactor, the estimations are nowhere as good. This stems from Eq. (26) in which r_0 is unknown; i.e., which is the characteristic generating dimension. Near the head r_0 could be taken as the radius of the injector tubes (1.32 mm) and away from the head as the radius of the reactor tubes (1.59 cm = 15.9 mm). Table II is constructed on this premise and as can be seen the comparison is only fair being more than an order of magnitude off for some terms.

For the mixing vessel, we have yet to attempt to estimate the parameters because of a lack of knowledge of r_0 (a guess at this time is blade width or radius) or a knowledge of the total kinetic energy.

To summarize, much has been learned about the simple (?) shear flow that occurs in a pipe. Reasonable estimates are available for the parameters of the statistical turbulence, but the same cannot be said for more complicated geometries.

TABLE I
PIPE FLOW

	3-inch H_2O, $r/r_o=0$		2-inch Trichloroethylene $r/r_o = 0$		0.35		0.70	
	exp	calc	exp	calc	exp	calc	exp	calc
r_0, cm	3.865		2.505					
ν, cm^2/sec	0.01		0.00374					
u_x', cm/sec	2.325		1.347					
k_0, cm^{-1}	0.70	0.5175	0.86	0.762	0.94	0.762	1.07	0.762
L_f, mm	14.2	14.5	12.1	9.84	8.8	9.84	5.4	9.84
λ, mm	2.23	2.36	1.62	1.58	1.44	1.46	1.19	1.29
ϵ, cm^2/sec	16.2	14.0	3.9	3.9	6.8	6.6	16.1	13.9

TABLE II
MULTIJET REACTOR

	NEAR HEAD		FAR FROM HEAD	
	exp	calc	exp	calc
r_0, mm	0.66		15.9	
ν, cm^2/sec	0.01		0.01	
u_x', cm/sec	13.8		13.8	
k_0, cm^{-1}	1.74#	30.3	0.24	1.25
L_1, L_f, mm	1.76, 1.85*	0.247	5.08, 9.00*	6.0
λ, mm	0.42	0.094	1.3	0.63
$\epsilon \times 10^{-4}$, cm^2/sec^3	5.2, 5.5+	109	0.12, 0.18+	0.72

\+ from Eq. (22) other from spectrum

* from Eq. (21)

\# from Eq. (25)

ACKNOWLEDGMENT

The senior author would like to acknowledge the help of his son Philip Arthur Brodkey who made the following contribution to replace the lost original manuscript of this paper:

Terbylenc

is caused when two
objects our rubed together
in a clockwise motion.
When you rub something
counterclockwise motion
it is called "nonterbylenc"

When you put water
in a paper cup and
rotate it, it is called
"licwedterbylenc"

When you take a
paper cup without water
in it and rotate it, it's called
"dryterbylenc"

Philip Arthur Brodkey
June 1960

SYMBOLS

A_i, B_i, C_i	constants
$f(\tau)$	autocorrelation
$F(u_x)$	flatness factor
i	summation index
k	wave number
k_0	wave number defined by Eq. 25
k_η	wave number defined by Eq. 24
L_f	macroscale
L_1, L_2, L_3	macroscales as defined in text
N	number
N(O)	number of zero crossings
$N_{Re,\lambda}$	Reynolds number defined by Eq. 23
$P(u_x)$	probability
r_x	transformed distance = $\tilde{U}_x t$
r_0	radius of pipe
s	actual signal = $au_x + \tilde{s}$
$S(u_x)$	skewness factor
t	time
u_x	instantaneous veldcity fluctuation
$\overline{u_x u_r}$, $\overline{u_r u_\theta}$	cross stress terms in turbulence
u'	rms velocity fluctuation in direction of flow
u_x', u_r', u_θ'	rms velocity fluctuations for pipe flow
U^*	friction velocity = $\sqrt{\tau_w/\rho}$
$\tilde{U}_x$	mean axial velocity
x, r, θ	pipe flow directions
ρ	density
ν	kinematic viscosity
τ	time delay
$\phi(k)$	one-dimensional spectrum
ϵ	kinetic energy dissipation
Δ	difference
Σ	sum
π	3.1416 ...
λ	microscale

REFERENCES

1. Brodkey, R. S., Fluid Motion and Mixing, Chap. 2 in Vol. 1 of Mixing: Theory and Practice, Uhl and Gray eds., Academic Press Inc., New York (1966).

2. Brodkey, R. S., The Phenomena of Fluid Motions, Addison-Wesley Publishing Company, Inc., Reading, Mass., 1967.

3. Nye, J. O., and Brodkey, R. S., "The Scalar Spectra in the Viscous-Convective Subrange," J. Fluid Mech., 29, 151 (1967).

4. Nye, J. O., and Brodkey, R.S., "Light Probe for the Measurement of Turbulent Concentration Fluctuations," Rev. Sci. Instr., 38, 26 (1967).

5. Gegner, J. P., and Brodkey, R. S., "Dye Injection at the Center-Line of a Pipe," A.I.Ch.E. J., 12, 817 (1966).

6. Brodkey, R. S., "Turbulent Motion and Mixing in a Pipe," A.I.Ch.E. J., 12, 403 (1966).

7. Lee, J., and Brodkey, R. S., "Turbulent Motion and Mixing in a Pipe," A.I.Ch.E. J., 10, 187 (1964).

8. Lee, J., and Brodkey, R. S., "Light Probe for the Measurement of Turbulent Concentration Fluctuations," Rev. Sci. Inst., 34, 1086 (1963).

9. Brodkey, R. S., Turbulent Motion, Mixing, and Kinetics, Prof. Dev. Lecture 1, #2, West Va. Univ., Kanawha Valley Grad. Center, Nitro, West Va. (1968).

10. Laufer, J. N.A.C.A. Report 1174 (1954).

11. Sandborn, V. A., N.A.C.A. T.N. 3266 (1955).

12. Brookshire, W. A., Ph.D. Thesis, La. State Univ., Baton Rouge, 1961.

13. Patel, R. H., McGill Univ. Tech. Note 63-6 (1963).

14. Patterson, G. K., Ph.D. Thesis, Univ. of Missouri, Rolla, Missouri (1966); also Patterson, G. K. and Zakin, J. L., A.I.Ch.E. J. 14, 434 (1968).

15. Rosler, R. S. and Priento, H. A., Chem. Eng. Sci., 23, 1219 (1968).

16. Iribarne, A., Hummel, R. L. Smith, J. W., and Frantisak, F., CEP Symp. Series No.91, 65, 60 (1969)

17. Bellhouse, B. J., and Schultz, D. L., J. Fluid Mech., 29, 289 (1967).

18. Hinze, J. O., Turbulence, McGraw-Hill, New York 1959.

19. Vassilatos, G., and Toor, H. L., A.I.Ch.E. J., 11, 666 (1965).

20. Grant, H. L., Stewart, R. W., and Moilliet, A., J. Fluid Mech., 12, 241 (1962).

21. Gibson, M. M., Nature, 195, 1281 (1962); J. Fluid Mech., 15, 161 (1963).

22. Cohen, M. F., M.S. thesis, The Ohio State University, Columbus (1962).

23. Knox, J. S., M. S. thesis, The Ohio State University, Columbus (1966).

24. McKee, G. L., M.S. thesis, The Ohio State University, Columbus (1966).

25. Rao, M. A., Ph.D. thesis, The Ohio State University, Columbus (1969).

26. McKelvey, K. N., Ph.D. thesis, The Ohio State University, Columbus (1968).

27. Zakanyez, S., Ph.D. thesis, the Ohio State University, Columbus (1971).

28. Yieh, H. C., Ph.D. thesis, The Ohio State University, Columbus (1970).